Patient-Specific Computer Simulation of Transcatheter Aortic Valve Replacement in Bicuspid Aortic Valve Morphology

Short Title: Dowling et al. Computer Simulation of TAVR in BAV.

Authors Names and Degrees: Cameron Dowling, MBBS,[a] Alessandra M. Bavo, PhD,[b] Nahid El Faquir, MD,[c] Peter Mortier, PhD,[b] Peter de Jaegere, MD, PhD,[c] Ole De Backer, MD, PhD,[d] Lars Sondergaard, MD, DMSc,[d] Philipp Ruile, MD,[e] Darren Mylotte, MD,[f] Hannah McConkey, MBBS,[g] Ronak Rajani, MD,[g] Jean-Claude Laborde, MD,[a] Stephen J. Brecker, MD[a]

Author Affiliations: From the [a]Cardiology Clinical Academic Group, St. George's, University of London and St. George's University Hospitals NHS Foundation Trust, London, United Kingdom; [b]FEops NV, Ghent, Belgium; [c]Department of Cardiology, Erasmus MC, Rotterdam, The Netherlands; [d]The Heart Center, Rigshospitalet, University of Copenhagen, Copenhagen, Denmark; [e]Department of Cardiology and Angiology II, University Heart Centre Freiburg-Bad Krozingen, Bad Krozingen, Germany; [f]Department of Cardiology, University Hospital Galway, Galway, Ireland; and [g]Cardiovascular Division, The Rayne Institute BHF Centre of Research Excellence, King's College London and St. Thomas' Hospital, London, United Kingdom.

Address for Correspondence:
Dr. Cameron Dowling
Department of Cardiology, St. George's Hospital
Blackshaw Rd, London, United Kingdom SW17 0QT
Telephone: +44-(0)20-8725-3556 / Fax: +44-(0)20-8725-0211
Email: Cameron.Dowling@stgeorges.nhs.uk

Total Word Count: 5350 words.

Abstract

Background: A patient-specific computer simulation of transcatheter aortic valve replacement (TAVR) in tricuspid aortic valve has been developed which can predict paravalvular regurgitation (PVR) and conduction disturbance. We wished to validate a patient-specific computer simulation of TAVR in bicuspid aortic valve (BAV) and to determine whether patient-specific transcatheter heart valve **(**THV**)** sizing and positioning might improve clinical outcomes.

Methods: A retrospective study was performed on TAVR in BAV patients that had both pre- and post-procedural computed tomography (CT) imaging. Pre-procedural CT imaging was used to create finite element models of the aortic root. Finite element analysis and computational fluid dynamics was performed. The simulation output was compared to post-procedural CT imaging, cineangiography, echocardiography and electrocardiograms. For each patient, multiple simulations were performed, in order to identify an optimal THV size and position for the patient's specific anatomical characteristics.

Results: A total of 37 patients were included in the study. The simulations accurately predicted the THV frame deformation (minimum diameter intraclass correlation coefficient [ICC] 0.84, maximum diameter ICC 0.88, perimeter ICC 0.91, area ICC 0.91), more than mild PVR (area under the receiver operating characteristic curve [AUC] 0.86) and major conduction abnormalities (new left bundle branch block or high-degree atrioventricular block) (AUC 0.88). When compared to the implanted THV size and implant depth, optimal patient-specific THV sizing and positioning reduced simulation-predicted PVR and/or markers of conduction disturbance.

Conclusions: Patient-specific computer simulation of TAVR in BAV may predict the development of important clinical outcomes, such as PVR and conduction abnormalities.

Patient-specific THV sizing and positioning may improve clinical outcomes of TAVR in BAV.

Key Words

Transcatheter Aortic Valve Replacement

Bicuspid Aortic Valve

Patient-Specific Modelling

Finite Element Analysis

Clinical Perspective

Transcatheter aortic valve replacement (TAVR) is increasingly being used to treat younger, lower-risk patients, many of whom have bicuspid aortic valve morphology (BAV). While outcomes of TAVR in BAV have improved with increased operator experience and newer-generation devices, it would be desirable to better identify patients who may be at risk for unfavourable clinical outcomes, such as paravalvular regurgitation and conduction disturbance. Furthermore, outcomes of TAVR in BAV could potentially be improved through better transcatheter heart valve (THV) sizing and positioning. In this retrospective study it was demonstrated that patient-specific computer simulation may be used to predict the development of paravalvular regurgitation and conduction disturbance. Furthermore, computer simulation may be used to optimise the THV size and position to the patient's specific anatomical characteristics, reducing simulation-predicted paravalvular regurgitation and/or conduction disturbance. Moving forward, this technology might be used by clinicians to better risk-stratify patients with BAV who are being considered for either TAVR or surgery. Furthermore, for patients undergoing TAVR, computer simulation might be used to guide THV sizing and positioning. Prospective clinical evaluation is warranted.

Summarizing Tweet

See how computer simulation may be used to predict paravalvular regurgitation and conduction disturbance after TAVR in bicuspid aortic valve

Introduction

Transcatheter aortic valve replacement (TAVR) continues to expand into younger, lower-risk patients, many of whom have bicuspid aortic valve morphology (BAV).[1] While clinical outcomes of TAVR in BAV were initially unfavourable, improvements have been made with increased operator experience and newer-generation devices.[2-4] Nonetheless, TAVR in BAV remains challenging, with an incidence of paravalvular regurgitation and new permanent pacemaker implantation which is higher than with surgery.[5-7] Thus, it would be desirable to better identify patients at risk for these unfavourable clinical outcomes. Furthermore, clinical outcomes of TAVR in BAV could potentially be improved through better transcatheter heart valve (THV) sizing and positioning. One potential solution to both of these problems is patient-specific computer simulation.

A patient-specific computer simulation of TAVR in tricuspid aortic valve morphology has been developed and validated (TAVIguide, FEops, Ghent, Belgium). The computer simulation can predict the THV frame deformation, severity of paravalvular regurgitation and development of major conduction abnormalities.[8-10]

In this study, we aimed to validate a patient-specific computer simulation of TAVR in BAV by comparing the output of computer simulations to post-procedural computed tomography (CT) imaging, cineangiography, echocardiography and electrocardiograms. We hypothesised that computer simulations would predict the THV frame deformation, the severity of paravalvular regurgitation and the development of major conduction abnormalities. Furthermore, we hypothesised that patient-specific THV sizing and positioning would improve predicted clinical outcomes of TAVR in BAV.

Methods

The data and materials used to conduct the research will not be made available to other researchers. A retrospective, study was performed in six European centres (St. George's Hospital, Erasmus MC, Rigshospitalet, University Heart Centre Freiburg-Bad Krozingen, St. Thomas' Hospital and University Hospital Galway) on patients with BAV who had undergone TAVR and had both pre- and post-procedural electrocardiographic-gated cardiac CT imaging. BAV was classified using the Sievers system.[11] The study was approved by institutional review committees and subjects gave informed consent.

Paravalvular Regurgitation and Conduction Disturbance Assessment

Peri-procedural cineangiography, transoesophageal and transthoracic echocardiograms were reviewed and paravalvular regurgitation graded using a 3-class grading system.[12] Peri-procedural electrocardiograms were reviewed, and major conduction abnormalities defined as the development of either new left bundle branch block, Mobitz Type II second-degree atrioventricular block or third-degree atrioventricular block.

Finite Element Analysis

Finite element models of the CoreValve, Evolut R, Evolut PRO (Medtronic, Minneapolis, MN) and Lotus (Boston Scientific, Marlborough, MA) THVs, that had been previously developed, were used.[8] In brief, frame morphology was derived from micro CT scanning (30 μm resolution). Strut width was obtained from optical microscopy, or based on data shared by the device manufacturer. Mechanical properties of the nickel titanium (Nitinol) frames were obtained though *in vitro* radial compression testing at body temperature, recording radial force throughout the compression cycle.

Patient-specific finite element models of the aortic root were constructed from pre-procedural CT scans (Mimics v18.0, Materialise, Leuven, Belgium). The aortic wall, leaflets and calcium were modelled with differing mechanical properties, as previously described.[10]

The finite element model of the implanted THV was positioned within the aortic root model. Finite element analysis was performed using Abaqus/Explicit (v6.12, Dassault Systèmes, Vélizy-Villacoublay, France; available from https://www.3ds.com). All steps of the procedure, including pre- and post-dilatation were modelled.

The finite element analysis output was overlaid with the post-procedure CT scan and then the depth of implant, as measured from the nadir of the non-coronary cusp to the inflow portion of the THV, was assessed. If there was significant malalignment (≥1 mm), the THV was repositioned and the process was repeated until the depth of implant from the finite element analysis output matched the post-procedure CT scan.

The simulation-predicted minimum diameter, maximum diameter, area, perimeter and eccentricity index of the THV frame were then recorded at the inflow portion, leaflet nadir, leaflet coaptation zone and leaflet commissures, as previously described.[8] The predicted dimensions from the computer simulations were then compared with the corresponding measurements obtained from the post-procedure CT scans.

Computational Fluid Dynamics Analysis

The blood domain was derived from the finite element analysis output and then computational fluid dynamics simulation was performed (OpenFoam v5.0, OpenCFD, Bracknell, United Kingdom) using a fixed pressure gradient of 32 mm Hg, a value which had been derived invasively from a population sample.[9] The resulting flow in the left ventricular outflow tract, expressed in mL/sec, was recorded. The predicted paravalvular regurgitation

from the computer simulations was then compared to the peri-procedural cineangiography, transoesophageal and transthoracic echocardiograms.

Conduction Disturbance Modelling

The force exerted on the patient anatomy was extracted from the finite element analysis output. A region of interest, demarcating the location of the left bundle branch was identified, as previously described.[10] The maximum pressure exerted by the THV on the region of interest (maximum contact pressure) and the percentage of the region of interest subject to pressure by the THV (contact pressure index) were then measured. The predicted maximum contact pressure and contact pressure index from the computer simulations were then compared to the post-procedural electrocardiographic findings.

Optimizing Clinical Outcomes

Patients who developed more than mild paravalvular regurgitation or major conduction abnormalities underwent additional simulations, targeting a THV implant depth of 0 mm (annular), 4 mm (standard) and 8 mm (deep). These simulations were then repeated with a larger and smaller THV. The results of the optimal simulation were then compared to the simulation matching the implanted THV size and position, as determined from the post-procedure CT scan.

Further Assessment of the Patient-Specific Computer Simulations

Additional computer simulations were performed in order to assess the discriminatory power of the model without usage of the post-procedural implant depth. Finite element analysis was performed targeting a 4 mm (standard) implant depth. Computation fluid dynamics and conduction disturbance modelling were then performed.

Statistical Analysis

Statistical analysis was performed with SPSS version 24.0 (IBM Corporation, Armonk, NY). Continuous variables are presented as mean ± SD and categorical variables as frequencies (percentage). Correlation was tested using a two-way mixed intraclass correlation coefficient (ICC).[13] Agreement was tested using a Bland-Altman plot with a ≤1 mm difference in mean minimum and maximum diameter measurements considered acceptable.[14] Discriminatory power was tested using the area under a receiver operating characteristic curve (AUC). Optimal cut-offs were determined using Youden's J statistic.[15] Means of two groups were compared using a paired sample t test with a P value <0.05 considered significant.

Results

Patient Characteristics

A total of 37 patients were included in the study. Patient characteristics are presented in Table 1. Patients were elderly (mean age 79.1 ± 14.0 years) and at intermediate risk for surgery (Society of Thoracic Surgeons Predicted Risk of Mortality 4.6 ± 3.0%). There was wide variation in bicuspid leaflet morphology and calcium distribution (Figure 1).

Frame Deformation

A representation of the finite element analysis output is presented in the Figure 2. The finite element analysis was reliable at predicting the THV minimum dimensions (ICC=0.84, 95% CI 0.74-0.90), maximum dimensions (ICC=0.88, 95% CI 0.84-0.92), perimeter measurements (ICC=0.91, 95% CI 0.87-0.9401), area (ICC=0.91, 95% CI 0.85-0.94) and eccentricity index (ICC=0.52, 95% CI 0.28-0.68). There was strong agreement between the

computer simulation and post-procedure CT measurements (mean difference in minimum diameter -0.9 mm, mean difference in maximum diameter 0.2 mm) (Figure 3).

There was no correlation between the aortic annulus eccentricity index and either the simulated (ICC=0.15, 95% CI -0.11-0.416) or post-procedure CT (ICC=0.16, 95% CI -0.17-0.46) THV eccentricity, as measured at the leaflet nadir.

Paravalvular Regurgitation

Paravalvular regurgitation severity was none in 10 patients (27.0%), mild in 15 patients (40.5%), moderate in 9 patients (24.3%) and severe in 3 patients (8.1%). Two patients required late re-intervention for paravalvular regurgitation and both were treated with post-dilatation. A representation of the computational fluid dynamics simulation is presented in Figure 4. The average simulation-predicted paravalvular regurgitation was 23.5 ± 32.5 mL/sec. Simulation-predicted paravalvular regurgitation was higher in patients who developed more than mild paravalvular regurgitation, when compared with patients who did not (49.8 ± 43.5 versus 10.8 ± 14.2 mL/sec, P<0.001). The computational fluid dynamics analysis demonstrated a discriminatory power to predict the development of more than mild paravalvular regurgitation (AUC=0.86, 95% CI 0.74-0.99, P<0.001) (Figure 5).

The optimal cut-off for discriminating none-to-mild from moderate-to-severe paravalvular regurgitation was a simulation-predicted paravalvular regurgitation of 13.6 mL/sec, representing a sensitivity of 92%, a specificity of 72%, a positive predictive of 61% and a negative predictive value of 95%.

Conduction Disturbance

The membranous septum could be identified in 20 cases which had adequate right-sided contrast enhancement and no pre-existing conduction disturbance. Major conduction

disturbance occurred in 15 (75.0%) of these cases (new left bundle branch block in 12 patients and third-degree atrioventricular block in 3 patients) and a permanent pacemaker was implanted in 5 of these patients (25.0%).

The average implant depth as measured at the non-coronary cusp was 4.6 ± 2.8 mm. The average implant depth was similar between patients who developed major conduction abnormalities and those who did not (5.0 ± 2.8 versus 3.5 ± 2.7 mm, P=0.33). The implant depth did not demonstrate any discriminative power to predict the development of major conduction abnormalities (AUC=0.72, 95% CI 0.45-0.99, P=0.14).

A representation of the contact pressure modelling is presented in Figure 6. The average maximum contact pressure was 0.73 ± 0.42 MPa. The maximum contact pressure was similar between patients who developed major conduction abnormalities and those who did not (0.76 ± 0.43 versus 0.64 ± 0.40 MPa, P=0.59). The maximum contact pressure did not demonstrate any discriminative power to predict the development of major conduction abnormalities (AUC=0.55, 95% CI 0.26-0.84, P=0.73).

The average contact pressure index was 0.20 ± 0.14%. The contact pressure index was higher in patients who developed major conduction abnormalities, when compared with those who did not (0.24 ± 0.15 versus 0.07 ± 0.04%, P=0.02). The contact pressure index demonstrated a discriminatory power to predict the development of major conduction abnormalities (AUC=0.88, 95% CI 0.73-1.00, P=0.01).

The optimal cut-off for discriminating the development of major conduction disturbance was a contact pressure index of 0.14, representing a sensitivity of 67%, a specificity of 72%, a positive predictive of 100% and a negative predictive value of 50%.

Patient-Specific Valve Sizing and Positioning.

An example of patient-specific THV sizing and positioning is presented in Figure 7. For the 12 patients who developed more than mild paravalvular regurgitation, the computer simulations suggested that predicted PVR would be reduced by altering the THV prosthesis size in 7 patients (58.3%), altering the implant depth in 8 patients (66.7%) and a combination of these strategies in 4 patients (33.3%). When compared with the simulation matching the implanted THV size and implant depth, optimal patient-specific THV sizing and positioning reduced simulation-predicted paravalvular regurgitation from 49.8 to 20.9 mL/sec (mean difference -28.9 mL/sec, 95% confidence interval [CI] -53.8 to -4.2 mL/sec, P=0.03). A standard and an annular implant depth were predicted to have a similar degree of PVR (46.3 ± 43.5 vs. 32.9 ± 21.4 mL/sec, P=0.30).

For the 15 patients who developed major conduction disturbance, the computer simulations suggested that predicted conduction disturbance would be reduced by altering the THV prosthesis size in 1 patient (6.7%) and altering the implant depth in 12 patients (80.0%). When compared with the simulation matching the implanted THV size and implant depth, optimal patient-specific THV sizing and positioning reduced simulation-predicted contact pressure index from 0.23 to 0.07 (mean difference -0.16, 95% CI -0.22 to -0.10, P<0.001). An annular implant depth was predicted to reduced contact pressure index when compared with a standard implant depth (0.08 ± 0.08 vs. 0.23 ± 0.14, P<0.001).

Further Assessment of the Patient-Specific Computer Simulations

When the computer simulations were performed without usage of the post-procedural implant depth, the discriminatory power of the paravalvular regurgitation modelling was similar (AUC, 0.81; 95% CI, 0.66-0.96; P=0.003), but the discriminatory power of the conduction disturbance modelling was lost (AUC, 0.55; 95% CI, 0.21-0.88; P=0.76).

Discussion

As TAVR expands from the extreme, high and intermediate-risk cohorts into younger, lower-risk patients, achieving optimal clinical outcomes in BAV will be important. More than mild paravalvular regurgitation may be associated with an increased risk of all-cause mortality, rehospitalisation and impaired functional status.[16] Left bundle branch block may be associated with a lack of improvement in left ventricular ejection fraction, impaired functional status, an increased risk of cardiac death and a higher risk for permanent pacemaker implantation.[17-22] Permanent pacemaker implantation may be associated with a longer duration of initial hospitalization, lack of improvement in left ventricular ejection fraction and an increased risk of late hospitalization or death.[22-24] Given the high standards of surgical aortic valve replacement, none of these clinical outcomes are desirable in a young, low-risk patient cohort.

In this study, we evaluated a patient-specific computer simulation of TAVR in BAV. We began by comparing finite element analysis with post-procedure CT scans, and confirmed that the computer simulations may accurately predict the THV frame deformation. We then compared computation fluid dynamics with peri-procedural imaging and established that the computer simulations may predict the development of more than mild paravalvular regurgitation. Next, we compared contact pressure modelling with peri-procedural electrocardiograms and confirmed that the computer simulations may predict the development of major conduction disturbance. Interestingly, our validation of the computer simulations identified optimal cut-offs for the development of more than mild PVR and major conduction abnormalities, which were very similar to previously reported values derived from work in tricuspid aortic valve morphology (simulation-predicted PVR of 16.25 mL/sec and a contact pressure index of 0.14).[9, 10]

Having validated these patient-specific computer simulations, clinicians might use this tool to better risk-stratify patients with BAV anatomy who are being considered for either TAVR or surgery. Patients in whom computer simulation predicts a favourable clinical outcome might be considered for TAVR, whereas for those in whom an unfavourable clinical outcome is expected, surgery may be the preferred treatment modality.

Currently, there is no widely accepted THV sizing algorithm for BAV. Strategies include annular, supra-annular and balloon-sizing methods.[25-28] Throughout the spectrum of BAV, there exists a broad range of potential leaflet configurations, intercommissural angles and calcium distribution. This heterogeneity has significantly hindered attempts to develop a bicuspid sizing algorithm. Furthermore, there is no widely accepted THV implant depth for BAV.

In this study we ran multiple simulations of varying THV sizes and positions, in order to identify an optimal THV size and implant depth for the patient's specific anatomical characteristics. This study demonstrated that patient-specific THV sizing and positioning may reduce simulation-predicted paravalvular regurgitation and/or markers of conduction disturbance. It is therefore plausible that patient-specific THV sizing and positioning might lead to improved clinical outcomes, but further prospective and randomized evaluation will be required to definitively prove this hypothesis.

In this study, post-procedural CT imaging was used to ensure that the computer simulations were performed at a comparable implant depth. When the simulations were performed without this information, the discriminatory power of the computational fluid dynamics analysis was similar, but the discriminatory power of the conduction disturbance modelling was lost. The development of conduction disturbance after TAVR is highly sensitive to implant depth.[29] Prospective evaluation is required to definitively establish the predictive power of the computer simulations.

In this study we found no correlation between aortic annulus eccentricity index and simulation-predicted or actual THV frame dimensions. This is consistent with previous observations that in bicuspid patients, maximal THV constraint occurs in the supra-annular complex.[25]

Limitations

The SAPIEN 3 THV (Edwards Lifesciences, Irvine, CA) has recently been reported to be associated with favourable clinical outcomes in bicuspid anatomy.[30] The computer simulations cannot currently simulate the SAPIEN 3 THV as we were unable to obtain this valve for micro CT scanning and radial compression testing. This study would be improved by the addition of this prosthesis. This study was small and retrospective and would be enhanced through a larger, prospective collection of both invasive measures of aortic regurgitation, such as the aortic regurgitation index, and better non-invasive measures of aortic regurgitation, such as phase-contrast velocity mapping with cardiac magnetic resonance imaging.[31, 32] The frequency of more than mild paravalvular regurgitation was high in this study. Paravalvular regurgitation may reduce over time and this study would be enhanced by long-term echocardiographic follow-up.[33] We were unable to assess whether there was any correlation between the location of simulation-predicted and observed PVR jets, as echocardiographic short axis views were not performed in a standardised manner. Only a limited number of CT scans were suitable to perform conduction disturbance modelling and therefore there were broad confidence intervals for the ability of the simulations to predict conduction disturbance. The finite element analysis modelling is currently unable to simulate important clinical complications such as aortic or ventricular embolization and aortic root rupture. Finally, the simulations do not predict post-procedure valvular gradients or aortic valve area.

Conclusion

Patient-specific computer simulation of TAVR in BAV may predict the development of important clinical outcomes, such as paravalvular regurgitation and conduction abnormalities. Computer simulation suggests that patient-specific THV sizing and positioning may improve clinical outcomes of TAVR in BAV.

Acknowledgments

This work has been presented as an abstract at EuroPCR 2018, Transcatheter Cardiovascular Therapeutics 2018 and the Cardiac Society of Australia and New Zealand Annual Scientific Meeting 2019.

Sources of Funding

No funding was received for this work.

Disclosures

Dr. Dowling has received grant support and speaker honoraria from Medtronic. Dr. Bavo is an employee of FEops. Dr. Mortier is a co-founder of FEops. Dr. De Backer has been a consultant for Abbott Vascular. Prof. Sondergaard has received consultant fees and institutional research grants from Abbott, Boston Scientific, Edwards Lifesciences and Medtronic. Prof. Brecker has received grant support, speaker honoraria and has served as a consultant to Medtronic and a consultant to Boston Scientific. All other authors have reported that they have no relationships relevant to the contents of this paper to disclose.

References

1. Roberts WC, Ko JM. Frequency by decades of unicuspid, bicuspid, and tricuspid aortic valves in adults having isolated aortic valve replacement for aortic stenosis, with or without associated aortic regurgitation. *Circulation*. 2005;111:920-925.

2. Mylotte D, Lefevre T, Sondergaard L, Watanabe Y, Modine T, Dvir D, Bosmans J, Tchetche D, Kornowski R, Sinning JM, et al. Transcatheter aortic valve replacement in bicuspid aortic valve disease. *J Am Coll Cardiol*. 2014;64:2330-2339.

3. Perlman GY, Blanke P, Dvir D, Pache G, Modine T, Barbanti M, Holy EW, Treede H, Ruile P, Neumann FJ, et al. Bicuspid Aortic Valve Stenosis: Favorable Early Outcomes With a Next-Generation Transcatheter Heart Valve in a Multicenter Study. *JACC Cardiovasc Interv*. 2016;9:817-824.

4. Yoon SH, Bleiziffer S, De Backer O, Delgado V, Arai T, Ziegelmueller J, Barbanti M, Sharma R, Perlman GY, Khalique OK, et al. Outcomes in Transcatheter Aortic Valve Replacement for Bicuspid Versus Tricuspid Aortic Valve Stenosis. *J Am Coll Cardiol*. 2017;69:2579-2589.

5. Colombo A, Latib A. Bicuspid aortic valve: any room for TAVR? *J Am Coll Cardiol*. 2014;64:2340-2342.

6. Guyton RA, Padala M. Transcatheter Aortic Valve Replacement in Bicuspid Aortic Stenosis: Early Success But Concerning Red Flags. *JACC Cardiovasc Interv*. 2016;9:825-827.

7. Makkar R, Chakravarty T, Jilaihawi H. Transcatheter Aortic Valve Replacement for Bicuspid Aortic Stenosis: Are We Ready for the Challenge? *J Am Coll Cardiol*. 2016;68:1206-1208.

8. Schultz C, Rodriguez-Olivares R, Bosmans J, Lefevre T, De Santis G, Bruining N, Collas V, Dezutter T, Bosmans B, Rahhab Z, et al. Patient-specific image-based computer simulation for theprediction of valve morphology and calcium displacement after TAVI with the Medtronic CoreValve and the Edwards SAPIEN valve. *EuroIntervention*. 2016;11:1044-1052.

9. de Jaegere P, De Santis G, Rodriguez-Olivares R, Bosmans J, Bruining N, Dezutter T, Rahhab Z, El Faquir N, Collas V, Bosmans B, et al. Patient-Specific Computer Modeling to Predict Aortic Regurgitation After Transcatheter Aortic Valve Replacement. *JACC Cardiovasc Interv*. 2016;9:508-512.

10. Rocatello G, El Faquir N, De Santis G, Iannaccone F, Bosmans J, De Backer O, Sondergaard L, Segers P, De Beule M, de Jaegere P, et al. Patient-Specific Computer Simulation to Elucidate the Role of Contact Pressure in the Development of New Conduction Abnormalities After Catheter-Based Implantation of a Self-Expanding Aortic Valve. *Circ Cardiovasc Interv*. 2018;11:e005344.

11. Sievers HH, Schmidtke C. A classification system for the bicuspid aortic valve from 304 surgical specimens. *J Thorac Cardiovasc Surg*. 2007;133:1226-1233.

12. Pibarot P, Hahn RT, Weissman NJ, Monaghan MJ. Assessment of paravalvular regurgitation following TAVR: a proposal of unifying grading scheme. *JACC Cardiovasc Imaging*. 2015;8:340-360.

13. Shrout PE, Fleiss JL. Intraclass correlations: uses in assessing rater reliability. *Psychol Bull*. 1979;86:420-428.

14. Bland JM, Altman DG. Statistical methods for assessing agreement between two methods of clinical measurement. *Lancet*. 1986;1:307-310.

15. Youden WJ. Index for rating diagnostic tests. *Cancer*. 1950;3:32-35.

16. Kodali S, Pibarot P, Douglas PS, Williams M, Xu K, Thourani V, Rihal CS, Zajarias A, Doshi D, Davidson M, et al. Paravalvular regurgitation after transcatheter aortic valve replacement with the Edwards sapien valve in the PARTNER trial: characterizing patients and impact on outcomes. *Eur Heart J*. 2015;36:449-456.

17. Houthuizen P, Van Garsse LA, Poels TT, de Jaegere P, van der Boon RM, Swinkels BM, Ten Berg JM, van der Kley F, Schalij MJ, Baan J, Jr., et al. Left bundle-branch block induced by transcatheter aortic valve implantation increases risk of death. *Circulation*. 2012;126:720-728.

18. Urena M, Webb JG, Cheema A, Serra V, Toggweiler S, Barbanti M, Cheung A, Ye J, Dumont E, DeLarochelliere R, et al. Impact of new-onset persistent left bundle branch block on late clinical outcomes in patients undergoing transcatheter aortic valve implantation with a balloon-expandable valve. *JACC Cardiovasc Interv*. 2014;7:128-136.

19. Regueiro A, Abdul-Jawad Altisent O, Del Trigo M, Campelo-Parada F, Puri R, Urena M, Philippon F, Rodes-Cabau J. Impact of New-Onset Left Bundle Branch Block and Periprocedural Permanent Pacemaker Implantation on Clinical Outcomes in Patients Undergoing Transcatheter Aortic Valve Replacement: A Systematic Review and Meta-Analysis. *Circ Cardiovasc Interv*. 2016;9:e003635.

20. Houthuizen P, van der Boon RM, Urena M, Van Mieghem N, Brueren GB, Poels TT, Van Garsse LA, Rodes-Cabau J, Prinzen FW, de Jaegere P. Occurrence, fate and consequences of ventricular conduction abnormalities after transcatheter aortic valve implantation. *EuroIntervention*. 2014;9:1142-1150.

21. Nazif TM, Williams MR, Hahn RT, Kapadia S, Babaliaros V, Rodes-Cabau J, Szeto WY, Jilaihawi H, Fearon WF, Dvir D, et al. Clinical implications of new-onset left bundle branch block after transcatheter aortic valve replacement: analysis of the PARTNER experience. *Eur Heart J*. 2014;35:1599-1607.

22. Jorgensen TH, De Backer O, Gerds TA, Bieliauskas G, Svendsen JH, Sondergaard L. Mortality and Heart Failure Hospitalization in Patients With Conduction Abnormalities After Transcatheter Aortic Valve Replacement. *JACC Cardiovasc Interv*. 2019;12:52-61.

23. Urena M, Webb JG, Tamburino C, Munoz-Garcia AJ, Cheema A, Dager AE, Serra V, Amat-Santos IJ, Barbanti M, Imme S, et al. Permanent pacemaker implantation after transcatheter aortic valve implantation: impact on late clinical outcomes and left ventricular function. *Circulation*. 2014;129:1233-1243.

24. Nazif TM, Dizon JM, Hahn RT, Xu K, Babaliaros V, Douglas PS, El-Chami MF, Herrmann HC, Mack M, Makkar RR, et al. Predictors and clinical outcomes of permanent pacemaker implantation after transcatheter aortic valve replacement: the PARTNER (Placement of AoRtic TraNscathetER Valves) trial and registry. *JACC Cardiovasc Interv*. 2015;8:60-69.

25. Liu X, He Y, Zhu Q, Gao F, He W, Yu L, Zhou Q, Kong M, Wang J. Supra-annular structure assessment for self-expanding transcatheter heart valve size selection in patients with bicuspid aortic valve. *Catheter Cardiovasc Interv*. 2018;91:986-994.

26. Xiong TY, Feng Y, Li YJ, Zhao ZG, Liao YB, Ou Y, Wei X, Chen M. Supra-Annular Sizing for Transcatheter Aortic Valve Replacement Candidates With Bicuspid Aortic Valve. *JACC Cardiovasc Interv*. 2018;11:1789-1790.

27. Jeger R, Reuthebuch O, Fahrni G, Laborde JC, Vogel R, Kaiser C. Supra-annular sizing for transcatheter valve implantation in bicuspid aortic stenosis. *Postepy Kardiol Interwencyjnej*. 2018;14:187-190.

28. Tchetche D, de Biase C, van Gils L, Parma R, Ochala A, Lefevre T, Hovasse T, De Backer O, Sondergaard L, Bleiziffer S, et al. Bicuspid Aortic Valve Anatomy and Relationship With Devices: The BAVARD Multicenter Registry. *Circ Cardiovasc Interv*. 2019;12:e007107.

29. Petronio AS, Sinning JM, Van Mieghem N, Zucchelli G, Nickenig G, Bekeredjian R, Bosmans J, Bedogni F, Branny M, Stangl K, et al. Optimal Implantation Depth and Adherence to Guidelines on Permanent Pacing to Improve the Results of Transcatheter Aortic Valve Replacement With the Medtronic CoreValve System: The CoreValve Prospective, International, Post-Market ADVANCE-II Study. *JACC Cardiovasc Interv*. 2015;8:837-846.

30. Makkar RR. Outcomes of transcatheter aortic valve replacement with balloon-expandable Sapien 3 valve in bicuspid aortic stenosis: an analysis of the STS/ACC TVT registry. Presented at: ACC 2019. March 17, 2019. New Orleans, LA.

31. Sinning JM, Hammerstingl C, Vasa-Nicotera M, Adenauer V, Lema Cachiguango SJ, Scheer AC, Hausen S, Sedaghat A, Ghanem A, Muller C, et al. Aortic regurgitation index defines severity of peri-prosthetic regurgitation and predicts outcome in patients after transcatheter aortic valve implantation. *J Am Coll Cardiol*. 2012;59:1134-1141.

32. Orwat S, Diller GP, Kaleschke G, Kerckhoff G, Kempny A, Radke RM, Buerke B, Burg M, Schulke C, Baumgartner H. Aortic regurgitation severity after transcatheter aortic valve implantation is underestimated by echocardiography compared with MRI. *Heart*. 2014;100:1933-1938.

33. Manoharan G, Van Mieghem NM, Windecker S, Bosmans J, Bleiziffer S, Modine T, Linke A, Scholtz W, Chevalier B, Gooley R, et al. 1-Year Outcomes With the Evolut R Self-Expanding Transcatheter Aortic Valve: From the International FORWARD Study. *JACC Cardiovasc Interv*. 2018;11:2326-2334.

Figures Legends

Figure 1. Representative sample of three-dimensional aortic valve reconstructions.

(A) A Sievers Type 0 (lateral) valve with moderate calcification. (B) A Sievers Type 0 (anterior-posterior) valve with heavy calcification. (C) A Sievers Type 1 (left-right raphe) valve with a heavily calcified raphe. (D) A Sievers Type 1 (right-non raphe) with a moderately calcified raphe.

Figure 2. Representation of the finite element analysis output.

(A) A patient with a Sievers Type 1 (left-right raphe) bicuspid valve has undergone patient-specific computer simulation. The output (B) demonstrates an elliptical THV that is constrained by the raphe, (C) leaflet and left ventricular outflow tract calcium. (D) The finite element analysis output correlates well with the (E) post-procedure computed tomography scan, as demonstrated by (F) the overlay.

Figure 3. Bland-Altman plots of the finite element analysis reliability at predicting the THV frame deformation.

Figure 4. Representation of the computational fluid dynamics simulation.

(A) The computation fluid dynamics simulation predicts a paravalvular regurgitation rate of 34.5 mL/sec, which correlates well with the (B) moderate paravalvular regurgitation seen on post-procedural transthoracic echocardiography.

Figure 5. Receiver operating characteristics curve for the ability of the computation fluid dynamics simulation to predict more than mild paravalvular regurgitation.

PVR = paravalvular regurgitation.

Figure 6. A representation of the contact pressure output.

The inferior border of the membranous septum is identified in three locations. (A) Near the non-coronary cusp. (B) The mid membranous septum. (C) Near the right coronary cusp. (D) The region of interest is defined by an area between the membranous septum (extended towards the right coronary cusp by 25°) and a plane 15 mm below the aortic annulus. The pressure exerted by the THV on the native anatomy is marked in purple. In this example the simulations predict both a high maximum contact pressure (0.58 MPa) and a high contact pressure index (0.47). The patient developed third-degree atrioventricular block after TAVR, necessitating permanent pacemaker implantation.

Figure 7. Patient-specific valve sizing and positioning to minimise paravalvular regurgitation. (A) A patient underwent TAVR with a 31 mm CoreValve, implanted at a standard implant depth. Computational fluid dynamics simulation predicts that there will be moderate paravalvular regurgitation (17.5 mL/sec). (B) The THV has been re-positioned at an annular level. Simulation predicts that paravalvular regurgitation severity will be reduced to mild (12.5 mL/sec).

Tables

Table 1. Patient characteristics.

Characteristic	**n=37**
Age, yrs	79.1 ± 14.0
Male	21 (56.8)
STS-PROM score	4.6 ± 3.0
Sievers classification	
Type 0	7 (18.9)
Lateral	2 (5.4)
Anterior-posterior	5 (13.5)
Type 1	30 (81.1)
Left-right raphe	26 (70.3)
Right-non raphe	3 (8.1)
Non-left raphe	1 (2.7)
Aortic root dimensions	
Left ventricular outflow tract (mm)*	25.9 ± 3.4
Aortic annulus (mm)*	25.9 ± 2.5
Aortic annulus eccentricity index	0.21 ± 0.07
Sinus of Valsalva (mm)*	36.3 ± 3.9
Sinotubular junction (mm)*	32.5 ± 4.2
Ascending aorta (mm)*	36.6 ± 4.4
THV prosthesis	
CoreValve	5 (13.5)

Evolut R	16 (43.2)
Evolut PRO	2 (5.4)
Lotus	14 (37.8)

* Perimeter-derived measurements

Values are mean ± SD or n (%).

STS-PROM = Society of Thoracic Surgeons Predicted Risk of Mortality.

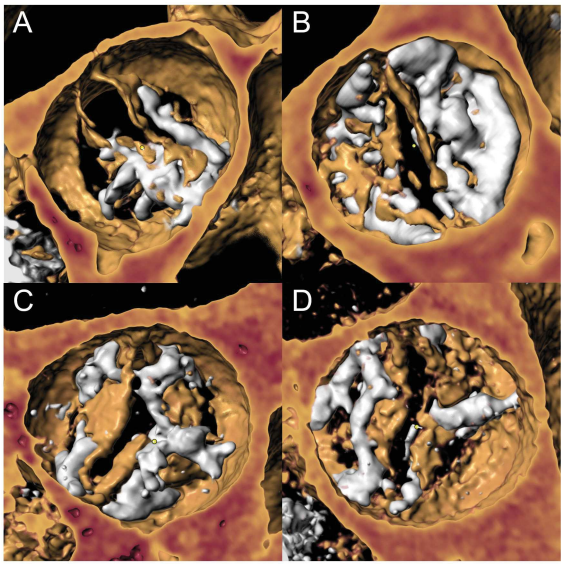
A
B
C
D

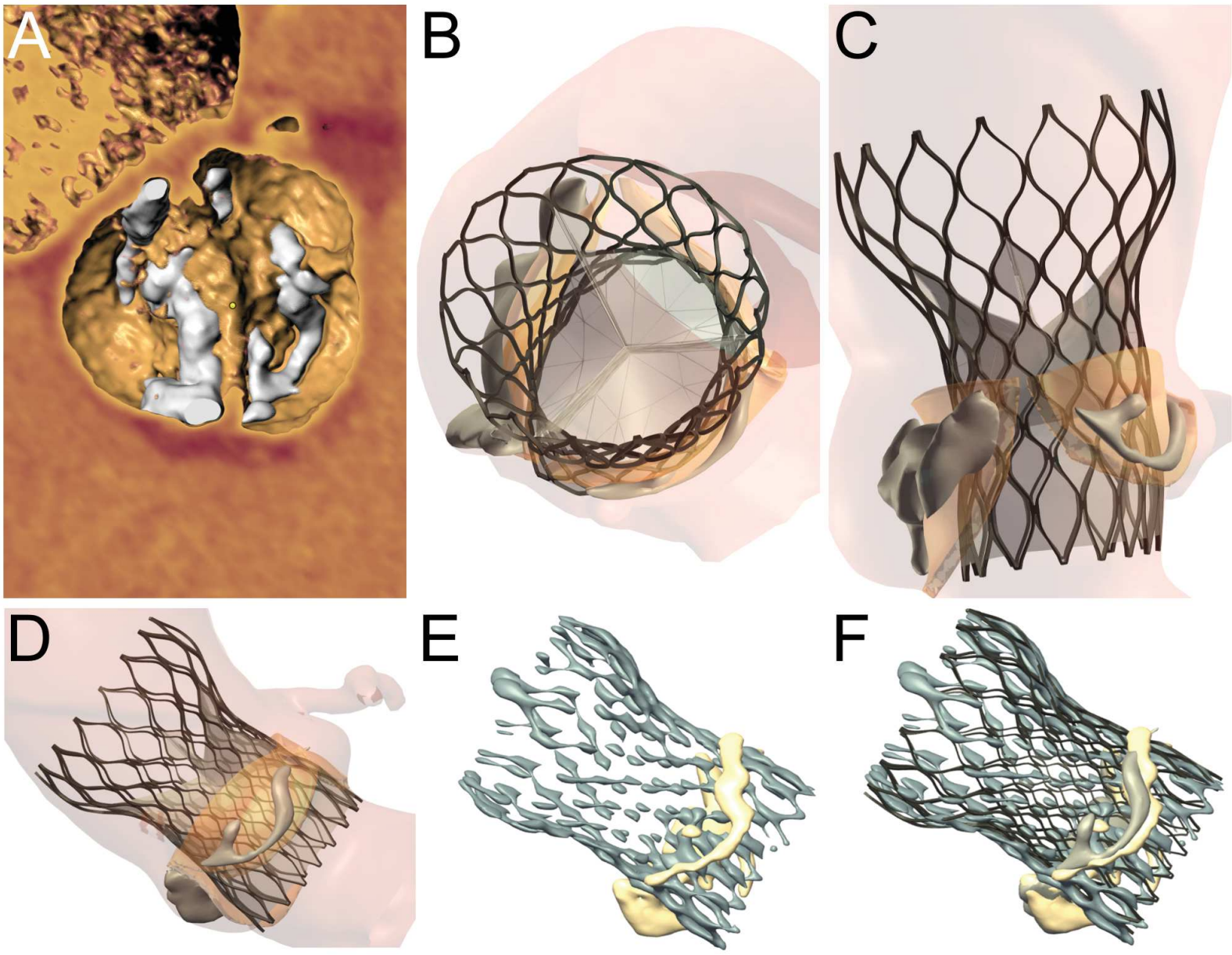
A
B
C
D
E
F

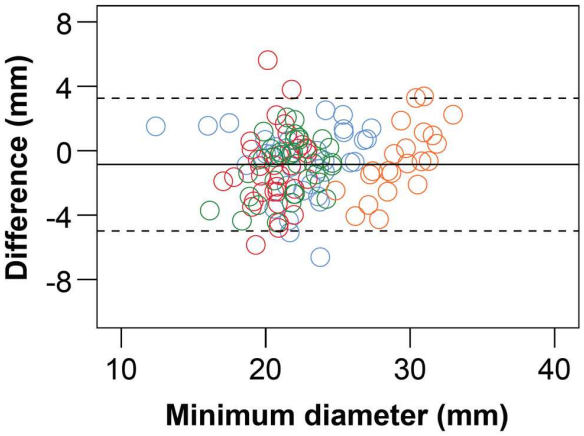
Difference (mm)
8
4
0
-4
-8
10
20
30
40
Minimum diameter (mm)

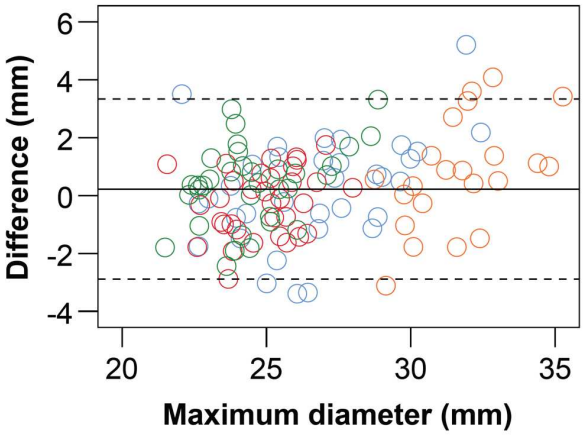
Difference (mm)
6
4
2
0
-2
-4
20
25
30
35
Maximum diameter (mm)

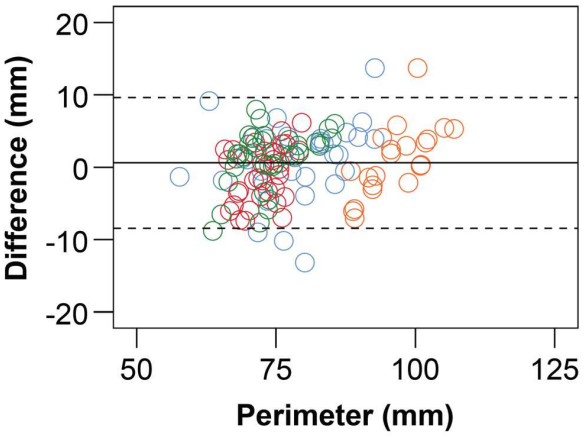
Difference (mm)
20
10
0
-10
-20
50
75
100
125
Perimeter (mm)

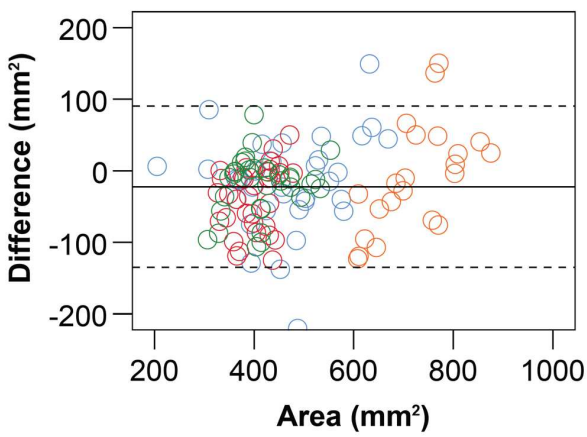
Difference (mm²)
200
100
0
-100
-200
200
400
600
800
1000
Area (mm²)


Measurement Location
Inflow
Leaflet nadir
Central coaptation zone
Commissures

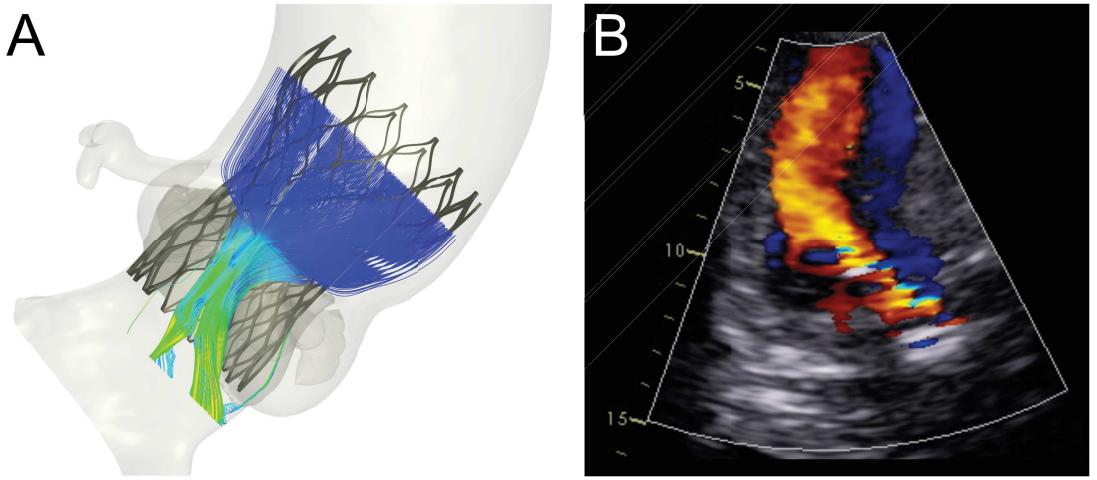
A
B
5
10
15

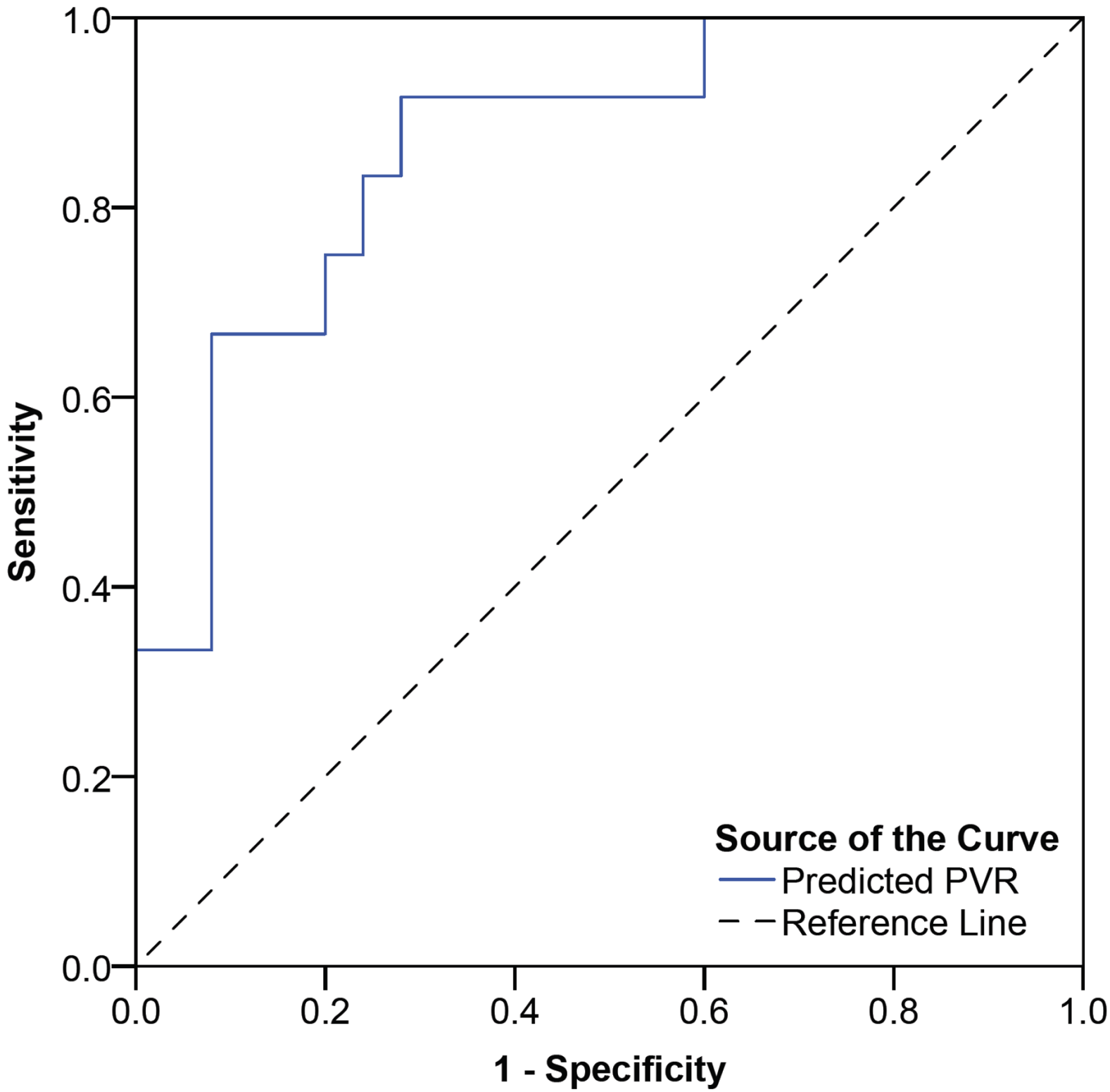
1.0
0.8
0.6
0.4
0.2
0.0
Sensitivity
0.0
0.2
0.4
0.6
0.8
1.0
1 - Specificity
Source of the Curve
Predicted PVR
Reference Line

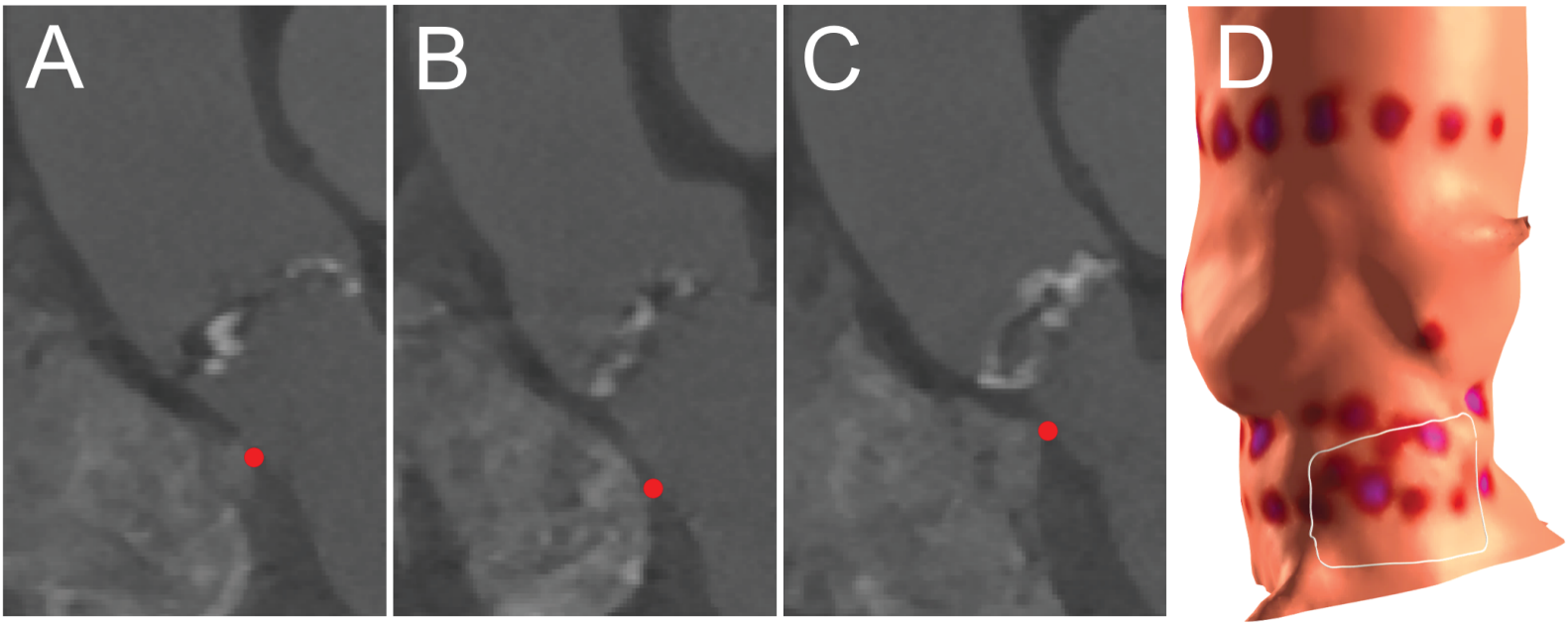
A
B
C
D

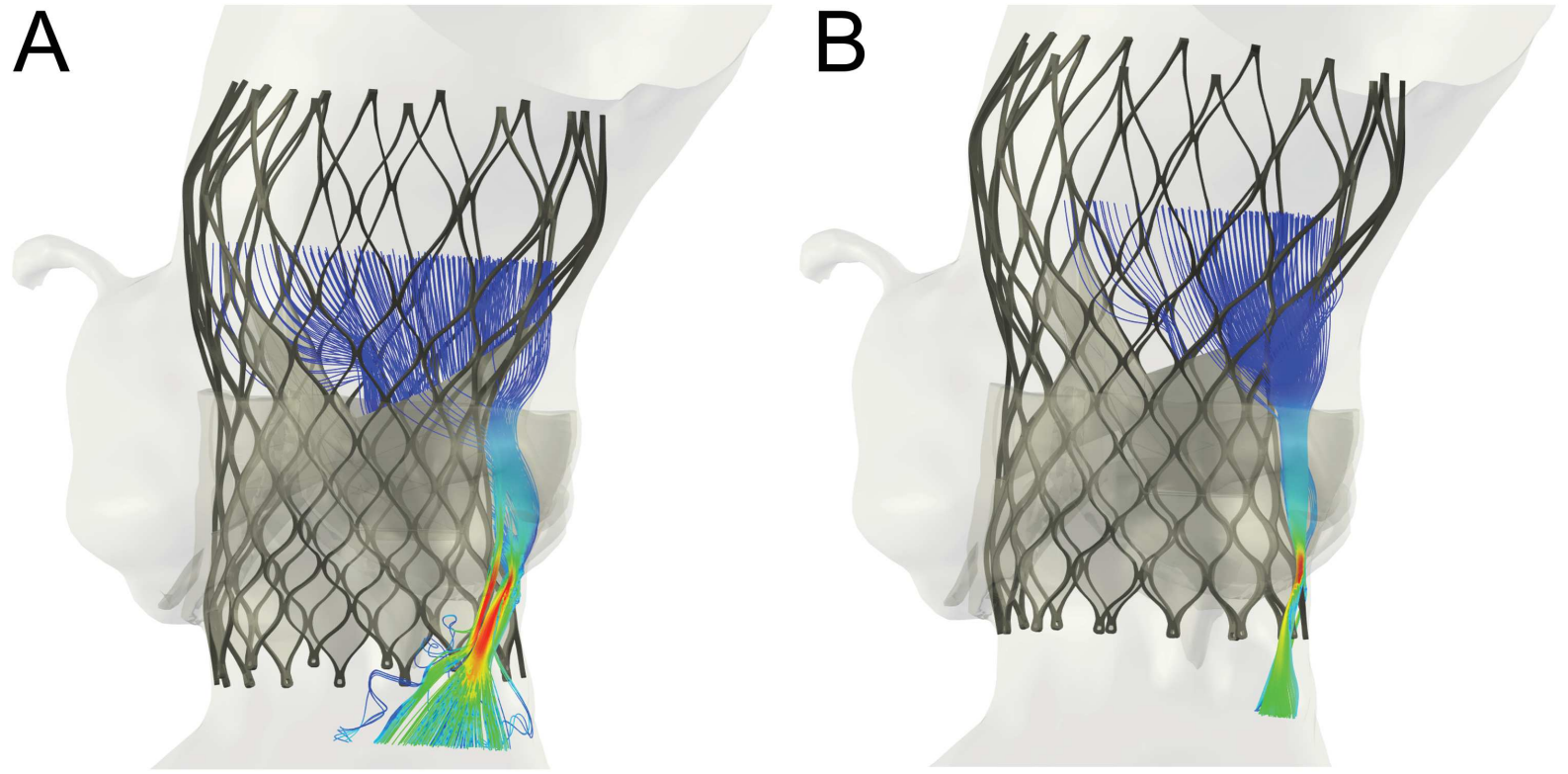
A
B